Journal of Sound and Vibration (2000) **230**(4), 915–932
doi:10.1006/jsvi.1999.2656, available online at http://www.idealibrary.com on IDEAL®

THE MEASUREMENT OF SOUND POWER FLUX IN FLOW DUCTS

K. R. HOLLAND AND P. O. A. L. DAVIES

Institute of Sound and Vibration Research, University of Southampton, Southampton SO17 1BJ, England

(*Received* 19 *May* 1999, *and in final form* 20 *September* 1999)

This paper describes the development of robust procedures yielding reliable estimates of the nett sound power flux associated with one-dimensional wave motion under strongly reactive conditions in flow ducts. In such reverberant situations, the measurements must be sufficiently precise to clearly identify the small fraction of the total fluctuating wave energy that is being propagated through the system [1–4]. An expansion chamber, together with its inlet and outlet pipes radiating into a semi-anechoic space, was chosen as a simple but sufficiently representative example of such systems. Various practical problems, such as those arising from low signal-to-noise ratios, or any inadequacies of microphone calibration were investigated in detail, along with various strategies for minimizing their influence on the realism and reliability of the associated measurements. The most effective procedures were identified by performing a sequence of comparisons between the resulting measurements and checking them against data generated with an existing and well-verified prediction code.

© 2000 Academic Press

1. INTRODUCTION

The noise from road traffic, and other land transport systems, has a major disturbing influence on the domestic environment. So also does noise from industrial, construction and agricultural processes and plant, where the sound emission from the exhaust and intake of an internal combustion engine often makes a significant contribution [1, 2]. Here, noise associated with the pulsating flow is often enhanced by vortex noise amplified by reverberation [3–8] or acoustic feedback. The coupled excitation of a tuned resonator by shed vorticity in a flowing fluid, often described as edge tone, has long been recognized as a primary generator of musical sound. Thus, in any reverberant situation, which includes tuned lengths of pipe, the rate of vortex shedding may be controlled by acoustic feedback [8] and thus synchronized by resonance, resulting in the coherent generation or amplification of sound.

The aeroacoustic generation of sound and its prediction has been a topic of active research, at least since the production of jet propelled aircraft, if not prior to this in the context of industrial and other transport activities. Furthermore, empirical studies of the production of musical sounds by wind instruments predate

0022-460X/00/090915 + 18 $35.00/0 © 2000 Academic Press

historical records. Although many of the basic physical mechanisms have been understood almost from the beginning, realistic quantitative predictions [3] have always relied on observed sound emissions either at model or full scale. In systems with complex geometry, such as intake or exhaust systems, or industrial pipe networks, the identification of the sources of acoustic excitation (and also of sound absorbers or sinks) involves local measurement of the associated acoustic characteristics including the sound power flux. It turns out that such measurements in flow ducts have presented severe problems in separating the flow-induced turbulent fluid dynamic pressure fluctuations or flow noise from those more coherent contributions generally associated with the acoustic wave motion.

There exists an extensive and rapidly expanding literature [2] describing sound propagation in exhaust systems, together with the associated prediction software packages; however, none of those currently available include quantitative estimates of the contributions of flow-generated noise to the predicted sound emissions. The increases in exhaust flow velocity, and thus flow noise, that accompany continuous development in engine performance, with the necessity of complying with ever more restrictive noise legislation, provide a strong incentive to improve quantitative understanding of the aeroacoustic and other relevant factors that influence flow noise generation in ducts. Observations have already demonstrated [3–8] that flow-induced resonance can be a generator of coherent sound, while similar mechanisms can provide selective amplification of existing acoustic excitation [5]. The first objective, which is the subject of this paper, is to produce reliable estimates of the coherent sound power flux at a sequence of stations along the flow path and, in particular, those that lie on either side of suspected sources of flow noise. However, the measurement of power flux in highly reactive systems at practically representative flow velocities was found to be fraught with difficulties. One significant factor is the presence of boundary layer and other flow-induced pressure fluctuations at the wall, while another is the low signal level that exists over those parts of the spectrum where the attenuation is high; the two factors combining to produce adverse signal-to-noise ratios. To concentrate on the first objective, and provide a baseline for future work, a flow duct configuration was chosen where coherent flow noise sources were expected to be negligible [5]. This was indeed borne out by the results of the measurements as is discussed in section 6.

2. THE DUCT SYSTEM

The duct system under investigation consists of a simple expansion chamber connected to inlet and outlet pipes, where Figure 1 shows the geometry, direction of flow and microphone positions. The inlet and outlet pipes are of polythene with 1 mm wall thickness, the expansion chamber of ABS with 3 mm wall thickness and the expansion chamber ends of plywood with 25 mm thickness. The component parts are securely glued and sealed together with silicone sealant.

Flow is provided by two electric fans via a large silencer chamber and is monitored using an orifice plate, calibrated against a traversed pitot-static tube. Acoustic excitation is via a loudspeaker horn compression driver attached to a side branch.

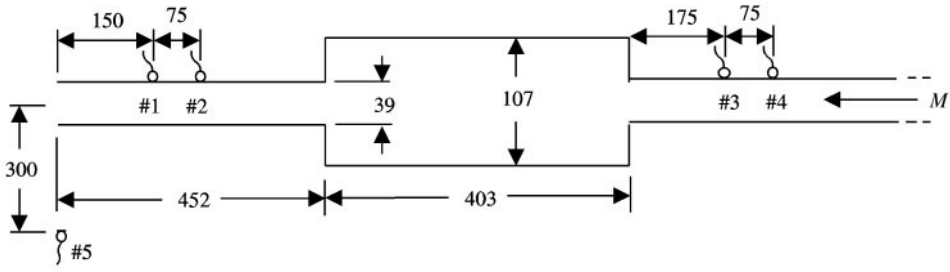

Figure 1. Geometry of duct system. Dimensions in mm.

3. MEASUREMENT METHOD

The two-microphone method, using a pair of flush-mounted wall microphones [9, 10], is a well-established and proven technique for estimating the acoustic properties of, and the acoustic quantities within, a duct system. It has been available ever since the development of digital signal acquisition and processing facilities in the early 1970s and provides a practical alternative to standing wave measurements. Initially, this method was applied successfully to the estimation of acoustic behaviour in uniform pipes at flow Mach numbers up to 0·3, [9] and 0·1 [10], combined with excitation levels well above those of the local boundary layer pressure fluctuations. Pairs of microphones are placed axially along each section of duct of interest, and the auto- and cross-spectra determined from the microphone pressure–time histories may then be processed to yield estimates of pressure spectra, forward and backward wave components, system transfer functions or sound power flux.

3.1. DETERMINATION OF WAVE COMPONENTS

Consider two microphones spaced a distance l apart. The fluctuating acoustic pressure at any point and frequency may be expressed as the sum of forward (in the direction of flow) and backward propagating wave components having complex spectral amplitudes $\hat{p}^+$ and $\hat{p}^-$ respectively. Thus, with one-dimensional waves,

$$\hat{p}(x, \omega) = \hat{p}^+ e^{-j\hat{k}^+ x} + \hat{p}^- e^{-j\hat{k}^- x}, \tag{1}$$

where, to first order in Mach number ($M = u_0/c_0$),

$$\hat{k}^+ = \frac{k + \alpha(1-j)}{(1+M)} \quad \text{and} \quad \hat{k}^- = \frac{k + \alpha(1-j)}{(1-M)} \tag{2a,b}$$

are the forward and backward complex wavenumbers respectively, $k = \omega/c_0$, α is the viscothermal attenuation coefficient defined as

$$\alpha = (1/ac_0)\,(\nu\omega/2)^{0\cdot5}\,[1 + (\gamma - 1)Pr^{-0\cdot5}], \tag{2c}$$

where a is the pipe radius, ν is the kinematic viscosity, γ is the ratio of specific heats, Pr is the Prandtl number, u_0 is the mean flow velocity and c_0 is the speed of sound. One reviewer pointed out that a more exact set of expressions than equations 2(a–c)

was available [11]. However, in the present case, the Stokes number, $a(\omega/\nu)^{0\cdot5}$, was sufficiently large that any errors resulting from the adoption of equations (2) rather than the more exact expressions, were always less than 0·02% and thus sufficiently small to be neglected.

Upon arbitrarily assigning $x = 0$ to be the position of microphone #1, the pressures at the two microphones may be written as

$$\hat{p}_1(\omega) = \hat{p}^+ + \hat{p}^- \quad \text{and} \quad \hat{p}_2(\omega) = \hat{p}^+ e^{-j\hat{k}^+ l} + e^{j\hat{k}^- l}. \tag{3a,b}$$

Let $\hat{G}_{12}$ be the cross-spectrum between the pressures at microphones #1 and #2 estimated from the time histories for the two microphones. From equation (3)

$$\hat{G}_{12} = \hat{p}_1^* \hat{p}_2 = (\hat{p}^+ + \hat{p}^-)^*(\hat{p}^+ e^{-j\hat{k}^+ l} + \hat{p}^- e^{j\hat{k}^- l}), \tag{4a,b}$$

and similarly, upon letting G_{11} be the autospectrum of the pressure at microphone #1,

$$G_{11} = \hat{p}_1^* \hat{p}_1 = (\hat{p}^+ + \hat{p}^-)^*(\hat{p}^+ + \hat{p}^-). \tag{5a,b}$$

Writing the complex ratio of the backward to forward pressure wave amplitudes as a complex pressure reflection coefficient at the position $x = 0$,

$$\hat{R} = \hat{p}^-/\hat{p}^+, \tag{6}$$

and dividing equation (4) by equation (5) yields

$$\frac{\hat{G}_{12}}{G_{11}} = \frac{e^{-j\hat{k}^+ l} + \hat{R} e^{-j\hat{k}^- l}}{1 + \hat{R}}. \tag{7}$$

from which the pressure reflection coefficient may be found in terms of the two measured quantities and the (assumed) known values of k, M and α, yielding

$$\hat{R} = -\left\{\frac{\hat{G}_{12} - G_{11} e^{-j\hat{k}^+ l}}{\hat{G}_{12} - G_{11} e^{j\hat{k}^- l}}\right\}. \tag{8}$$

Alternatively, the quantity $\hat{G}_{12}/G_{11}$ in equation (7) can be expressed as the H_1 transfer function $\hat{H}_{12} = \hat{p}_2/\hat{p}_1$, upon rewriting equation (8) as

$$\hat{R} = -\left\{\frac{\hat{H}_{12} - e^{-j\hat{k}^+ l}}{\hat{H}_{12} - e^{j\hat{k}^- l}}\right\}. \tag{8a}$$

From equations (5) and (6),

$$|\hat{p}^+| = \frac{(G_{11})^{1/2}}{|1 + \hat{R}|} \quad \text{and} \quad \hat{p}^- = \hat{R}\hat{p}^+. \tag{9a,b}$$

The fact that equation (9a) yields only the modulus of $\hat{p}^+$ does not matter as the phase of $\hat{p}^+$ can arbitrarily be chosen as zero without loss of generality, while $\hat{p}^-$ is complex in general. The phase of the pressure components derived from other microphone pairs in the system, relative to that at a single chosen reference microphone (#1), can then be determined by measuring the cross-spectrum or

transfer function between one microphone of the pair and microphone #1: thus,

$$\hat{p}^{\pm}_{n(ref)} = \hat{p}^{\pm}_{n} \hat{H}_{1n} \frac{(\hat{p}^{+}_{1} + \hat{p}^{-}_{1})}{(\hat{p}^{+}_{n} + \hat{p}^{-}_{n})} \quad \text{or} \quad \hat{p}^{\pm}_{n(ref)} = \hat{p}^{\pm}_{n} \frac{\hat{G}_{1n}}{(\hat{p}^{+}_{1} + \hat{p}^{-}_{1})^{*}(\hat{p}^{+}_{n} + \hat{p}^{-}_{n})}. \quad (10a,b)$$

One should note that the effectiveness of the decomposition depends upon how coherent the quantities $\hat{p}^{+}$ and $\hat{p}^{-}$ are, since the presence of flow-induced or other incoherent noise will compromise the resultant spectral estimates. Also, the two-microphone method relies upon differences between the pressure signals at the two microphones. Upon ignoring propagation losses and flow, the two pressure signals are identical when $kl = n\pi$, where n is any integer; the method will yield poor results when the distance between the microphones is close to multiples of half an acoustic wavelength. It is recommended that the spacing between the microphones be kept to within a half wavelength of the highest frequency of interest. A plane-wave assumption is inherent in the above analysis; for a uniform duct with steady, uniform flow, this limits the upper frequency of application to that corresponding to a Helmholtz number given by $ka < 1{\cdot}84(1 - M^2)^{0{\cdot}5}$.

3.2. DETERMINATION OF SOUND POWER FLUX

Two methods may be used to determine the sound intensity and hence sound power flux in a section of the duct. In one, a finite-difference approximation is used to determine the sound pressure and particle velocity at a plane between two closely spaced microphones; the sound intensity is then derived from an estimate of the cross-spectrum between the two microphones (see reference [12]); thus

$$I_T = \left[\frac{(1 - M^2)(1 + 3M^2)}{\rho_0 \omega l}\right] \mathrm{Im}\{\hat{G}_{12}\} + \left[\frac{M(1 + M^2)}{2\rho_0 c_0}\right](G_{11} + G_{22} + 2\mathrm{Re}\{\hat{G}_{12}\})$$

$$+ \left[\frac{Mc(1 - M^2)}{\rho_0 \omega^2 l^2}\right]\left[\frac{(G_{11} - G_{22})^2 + 4(\mathrm{Im}\{\hat{G}_{12}\})^2}{G_{11} + G_{22} + 2\mathrm{Re}\{\hat{G}_{12}\}}\right]. \quad (11)$$

In the second method, the sound intensity is calculated from the forward and backward pressure wave components estimated by using equations (8) and (9) above (see reference [13]); thus, for sufficiently large Stokes numbers and high Reynolds numbers,

$$I_T = I^{+} - I^{-} = (1/\rho_0 c_0)\,(|\hat{p}^{+}|^2(1 + M)^2 - |\hat{p}^{-}|^2(1 - M)^2), \quad (12a,b)$$

to a close approximation. The second method does not require closely spaced microphones as it relies on a sort of wavenumber curve fit between the microphones rather than the linear gradient approximations of the first method. It is shown in section 5.2 that, for the system under consideration here, the two methods yield similar results except at the highest frequencies.

3.3. CHOICE OF MICROPHONE POSITION

The microphones used to monitor the pressures within the duct system may be either mounted in the flow, or in the duct wall. Use of the former positions yields an output signal which is dominated by high levels of flow-induced noise due to the finite size of the microphone; such noise would not exist in the absence of the microphone and is therefore of no interest. Attempts to shield the microphones from the flow by using porous layers for example, leads to flow-dependent microphone sensitivity and therefore calibration difficulties; the resultant larger structure may also affect the flow. Mounting the microphones in, and flush with, the duct wall removes this problem, but high levels of boundary layer noise are still present. The latter method has been chosen for these investigations, using miniature electret microphones close coupled to short (3 mm long) 1 mm outside diameter probe tubes flush-mounted in the wall. The resonance frequency of the Helmholtz resonator set up between the cavity in front of the microphone and the probe tube was approximately 5 kHz which is outside the frequency range of interest.

The optimum axial position for the microphones depends upon the duct system under test, and on the acoustic quantities of interest. When considering plane impedance discontinuities with zero flow, such as samples in an impedance tube, it is good practice to mount the microphone pair close to the plane where the acoustic properties are required [14]. However, mounting the microphones too close to non-planar discontinuities, such as changes in cross-sectional area, invalidates the plane-wave assumptions due to the presence of evancescent near field pressure fluctuations associated with higher order duct modes. Furthermore, in the presence of flow, such discontinuities give rise to flow-induced pressure fluctuations which are also generally localized close to the discontinuity. For these reasons, it is recommended that the nearest microphone be mounted at least three pipe-diameters from any area discontinuity such as an open pipe-end.

3.4. MICROPHONE CALIBRATION

The acoustic field within a duct system is necessarily highly reactive at the low Helmholtz numbers (ka) of interest, thus the phase, and hence the imaginary part, of the cross-spectra used in the estimation of power flux is very close to zero over much of the frequency band. Accurate, *in situ* calibration of the microphones is therefore crucial to the success or otherwise of the subsequent measurement methods (see, for example, reference [10]). The calibration method chosen involves physically interchanging each pair of microphones. Firstly, the two microphones are placed in position and the transfer function between their outputs is measured yielding $\hat{H}_A$. The two microphones are then interchanged, including all signal path elements (recorder channel, amplifier, etc.) and the measurement repeated yielding $\hat{H}_B$. The required (calibration independent) transfer function of interest is then $\hat{H} = (\hat{H}_A \hat{H}_B)^{0{\cdot}5}$. The phase of the square root of the product of the two measurements is, in general, ambiguous (due to the possibility of wrapping); so to avoid such complications, the square roots should be evaluated prior to the

product; thus

$$\hat{H} = \hat{H}_A^{0\cdot5}\hat{H}_B^{0\cdot5} \quad \text{where} \quad \hat{H}_i^{0\cdot5} = |\hat{H}_i|^{0\cdot5} \exp(\mathrm{j}\arg(\hat{H}_i)/2). \tag{13}$$

Wrapping cannot then occur as the sum of the phases of the two square-rooted measurements will always be less than 2π. This method is repeated for each pair of microphones in turn yielding relative microphone calibration data. The (approximate) absolute calibration of one microphone only is then required if absolute sound pressure levels are important.

4. DATA ACQUISITION AND ANALYSIS METHOD

The output signals from the five microphones were recorded onto a multi-track digital tape recorder which was then played back into a multi-channel computer data acquisition system and stored as 16-bit data. This method gives freedom for experimentation with various data analysis methods and was therefore preferred, in this case, over the use of a dedicated multi-channel analysis package. All analysis was carried out using custom-written code on a 200 MHz RISC computer. The use of adequate frequency resolution in the analysis is important if bias errors are to be minimized [14]. A frequency resolution of 1 Hz was found to yield the optimum compromise between analysis time and bias error, through studies of the coherence function associated with the transfer function measurements. Ten minutes of data was analyzed for each measurement run, giving rise to 1200 process averages with Hanning windowing and 50% overlap. An analogue anti-aliasing filter set having a cut-off frequency of 1300 Hz was employed throughout these tests; data above this frequency are therefore deemed unreliable.

4.1. RANDOM EXCITATION

Experiments were carried out using a white noise signal as input to the loudspeaker. This form of acoustic excitation is commonplace in both static and flow acoustic studies and is the automatic "first choice" broadband test signal. Figure 2(a) shows the H_1 transfer function ($\hat{p}_2/\hat{p}_1$) measured between microphones $\#1$ and $\#2$ of the duct system using white noise excitation with a flow Mach number $M = 0{\cdot}1$, while Figure 2(b) shows the coherence function for the measurement. The sound pressure level of the acoustic signal at microphones $\#1$ and $\#2$ was 131 dB SPL which was greater than 10 dB above that of the boundary layer noise.

As the microphones were mounted close to a simple open pipe-end, one would expect the transfer function between them to be a relatively simple function of frequency. This is not the case in Figure 2(a), and inspection of the coherence (Figure 2(b)) reveals only limited bands of frequencies over which the measured result can be considered valid. Clearly, although the r.m.s. level of the acoustic excitation was much larger than that of the boundary layer noise, the wide variations in acoustic level with frequency at the exit of a resonant expansion chamber yield inadequate signal-to-noise ratios over much of the bandwidth. As

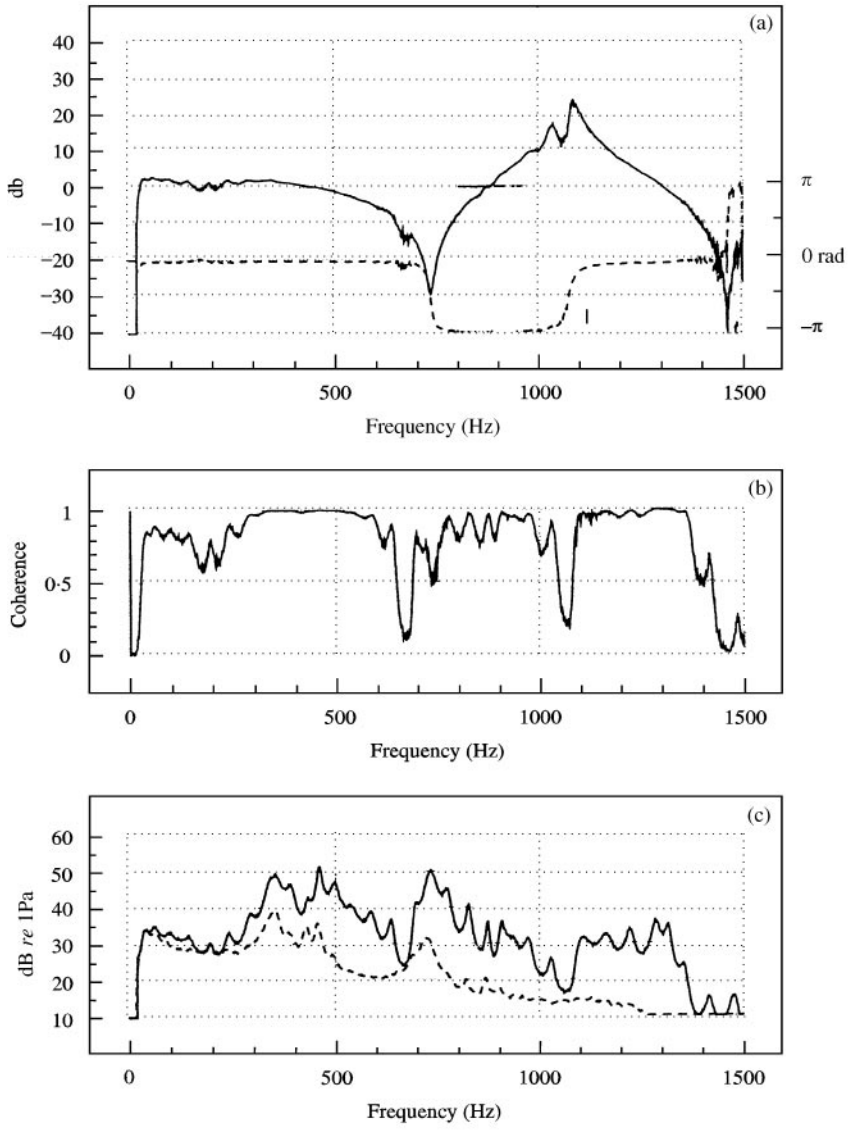

Figure 2(a). Modulus (——) and phase (– – –) of transfer function $\hat{H}_{12}$ measured when using random excitation with Mach Number $M = 0{\cdot}1$; (b) Coherence function for measurement in 2(a). (c) Autospectrum of output of microphone $\#1$ for measurement in 2(a) with acoustic excitation (——) and without (– – –).

the acoustic signal and the boundary layer noise are both random, separation of the two is difficult. Figure 2(c) shows the autospectrum of the output from microphone $\#1$ with and without acoustic excitation. A comparison between these and Figure 3(c) (see section 4.2) shows that the dips in acoustic signal level are buried in the noise floor. Raising the acoustic excitation level to help overcome the signal-to-noise ratio problem is impractical for three reasons: the loudspeaker may overload; the microphones may overload; and the propagation of acoustic waves

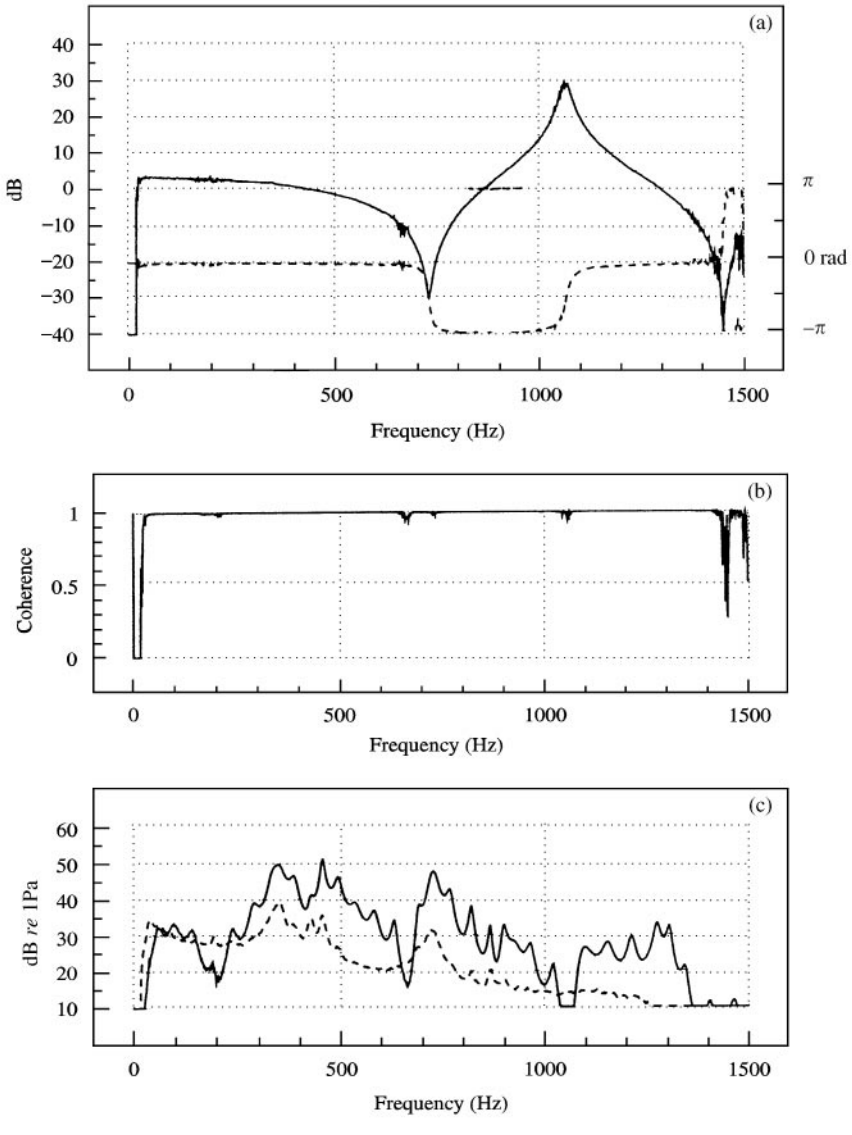

Figure 3(a). Modulus (——) and phase (– – –) of transfer function $\hat{H}_{12}$ measured using swept-sine excitation with selective averaging: mach number $M = 0{\cdot}1$. (b) coherence function for measurement in 3(a). (c) autospectrum of output of microphone $\#1$ for measurement in 2(a) with acoustic excitation (——) and without (– – –).

will become non-linear. Results such as that shown in Figure 2 are unacceptable for acoustic power flux estimation; a more precise method has been devised which utilizes a slow sine-sweep signal.

4.2. SINE-SWEEP EXCITATION

In an attempt to overcome the signal-to-noise ratio problems encountered using random noise excitation, a slow sine-sweep signal was used to excite the duct

system. This signal was generated digitally and recorded onto one channel of the digital tape; the remaining channels were then used to record the pressure signals from the microphones. Thus, the excitation signal and the resulting pressure signals were always synchronous in time. Furthermore, it was then relatively easy to tailor the digitally generated signal so that the sweep rate varied with time; setting a slower sweep rate at low frequencies, where the signal-to-noise ratio is poorest, resulted in improvements in the results at low frequencies. It is also possible to tailor the amplitude of the signal to improve the signal-to-noise ratio at some frequencies, although this was not attempted for the measurements described herein. Because the frequency of the sweep is known at any particular point in time, it is possible to exclude from the averaging process all frequencies except those within a narrow band around the known centre frequency. This temporally synchronous, frequency-exclusive, averaging process is latter referred to as selective averaging. Figure 3(a) shows the results of carrying out analysis of this nature on the microphone output signals with excitation in the form of a 10 min swept-sine signal and a flow Mach number $M = 0{\cdot}1$. The sound pressue level of the acoustic excitation varied with frequency between 100 and 140 dB at microphones $\#1$ and $\#2$; the overall time-averaged level being 131 dB; Figure 3(b) shows the coherence function for this measurement, and Figure 3(c) the autospectrum of the output of microphone $\#1$ with and without acoustic excitation.

A comparison between Figure 2, using random excitation and conventional analysis, and Figure 3, using swept-since excitation and selective averaging, shows that it is possible to separate out the required acoustic signal from the random boundary layer noise by using swept-sine techniques, even when the signal-to-noise ratio is much less than unity.

5. COMPARISON BETWEEN MEASUREMENTS AND PREDICTIONS

Computer codes exist for the prediction of the acoustic properties of ducts with flow. The predictions of one such code (APEX, with an appropriately modified output; see reference [1, 2]), written by the second author are presented below for comparison with the measured results. Good agreement between the predictions and measurements is assumed to validate both the code and the measurement technique.

5.1. ACOUSTIC TRANSFER FUNCTIONS

Figure 4(a) shows a comparison between the predicted and measured transfer functions $\hat{H}_{13}$ between microphones $\#1$ and $\#3$ with zero flow using swept-sine excitation and selective averaging. Figures 4(b) and 4(c) are as Figure 4(a) but for flow Mach numbers (M) of 0·1 and 0·2 respectively. Figures 5(a)–5(c) show similar comparisons between the predicted and measured transfer functions $\hat{H}_{15}$ between microphone $\#1$ and the free field microphone $\#5$ with zero flow and Mach numbers of 0·1 and 0·2 respectively. The somewhat ragged appearance of the measured results is probably due to room effects; the experiments were carried out

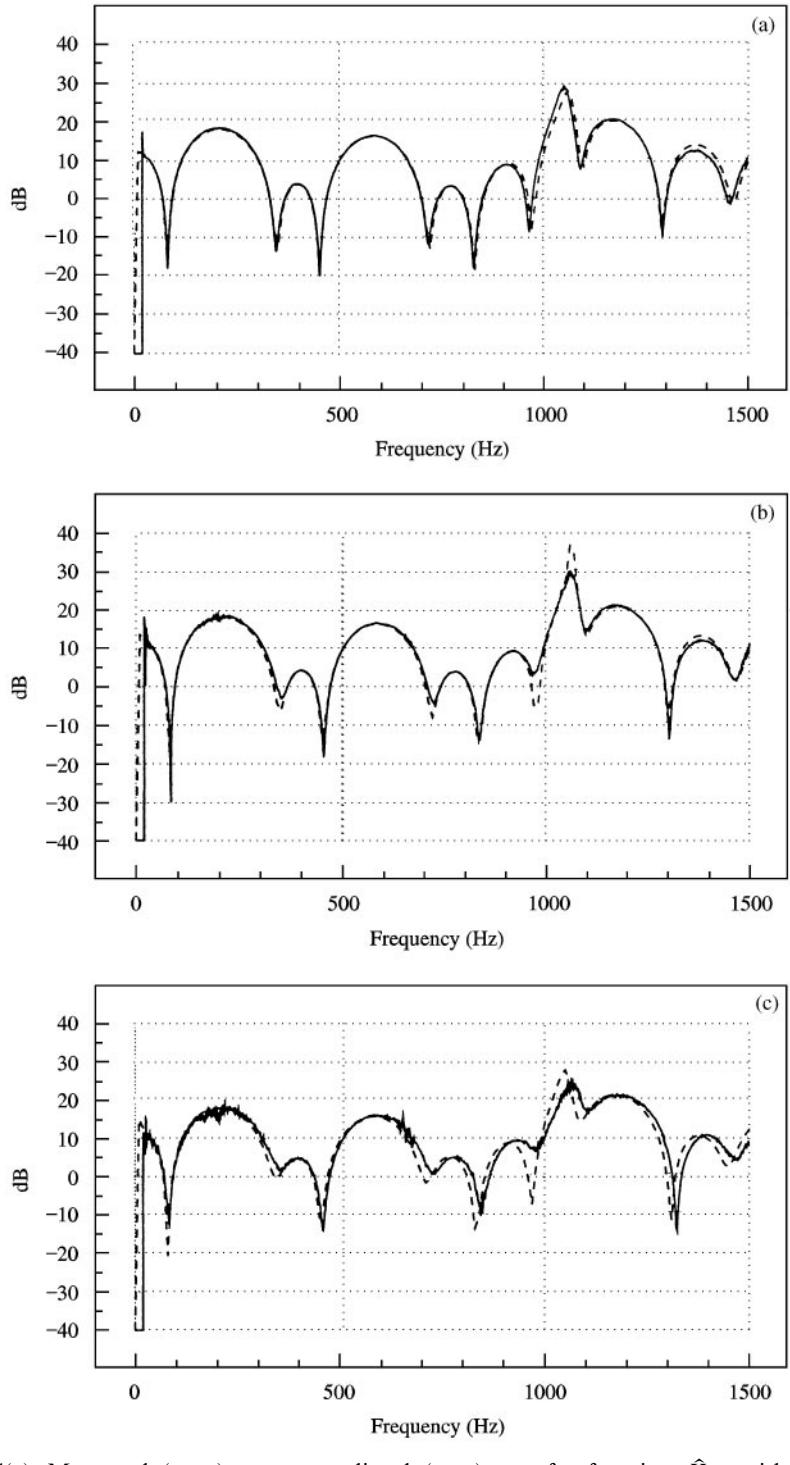

Figure 4(a). Measured (——) versus predicted (– – –) transfer function $\hat{H}_{13}$ with zero flow; (b) measured (——) versus predicted (– – –) transfer function $\hat{H}_{13}$ with Mach number $M = 0{\cdot}1$. (c) measured (——) versus predicted (– – –) transfer function $\hat{H}_{13}$ with Mach number $M = 0{\cdot}2$.

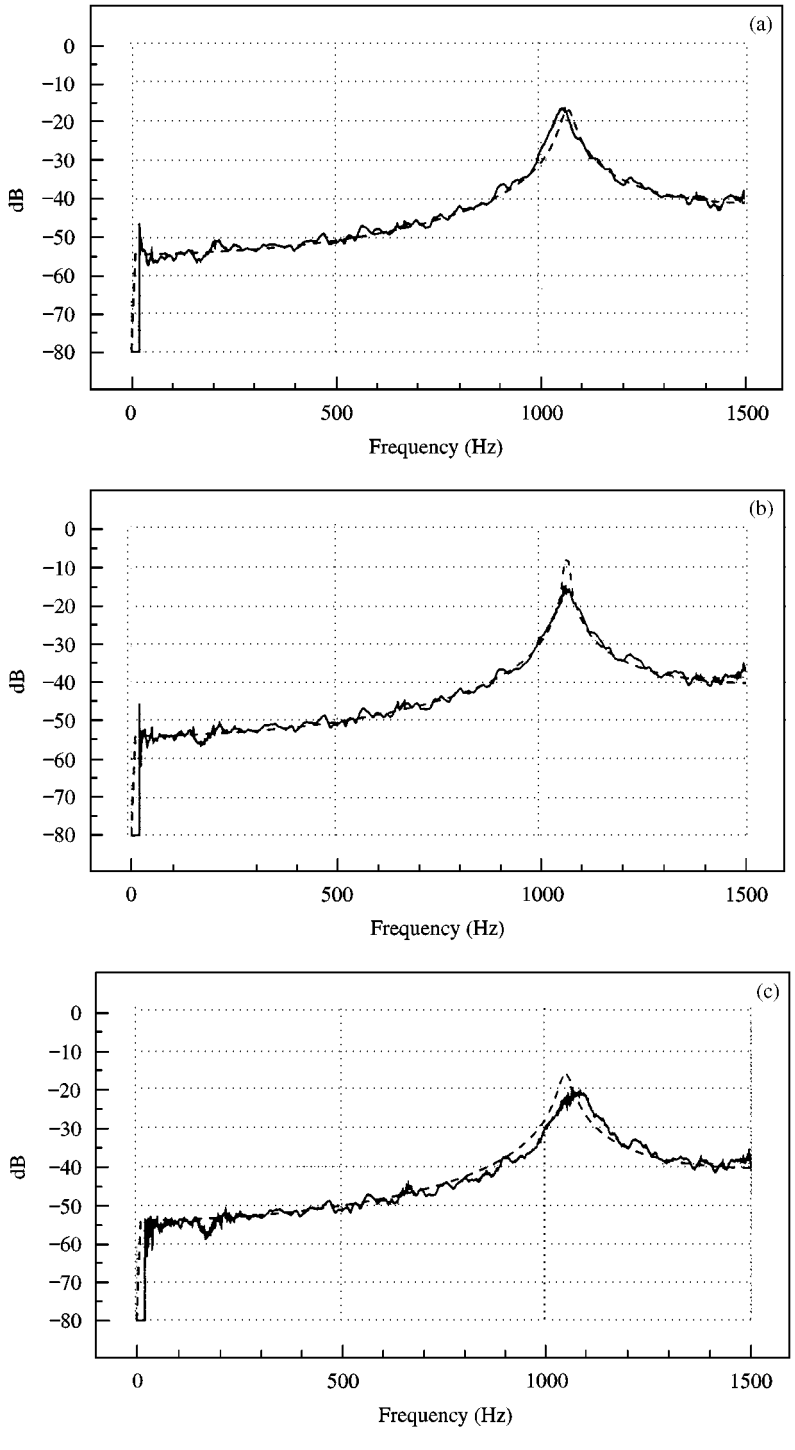

Figure 5(a). Measured (——) versus predicted (– – –) transfer function $\hat{H}_{15}$ with zero flow; (b). measured (——) versus predicted (– – –) transfer function $\hat{H}_{15}$ with Mach number $M = 0{\cdot}1$; (c). measured (——) versus predicted (– – –) transfer function $\hat{H}_{15}$ with Mach number $M = 0{\cdot}2$.

in a large, acoustically "dead", but non-anechoic laboratory, with a layer of absorbent wedges on the floor under the open termination.

5.2. ACOUSTIC POWER FLUX

The measured transfer functions were used to estimate the forward and backward pressure wave components by using equations (9), from which the net acoustic power flux may be estimated according to equation (12). For clarity and ease of comparison, all power flux results and predictions are normalized to the forward (with-flow) acoustic power (I^+) in the inlet pipe. Figures 6–8 respectively show comparisons between the predicted and measured normalized acoustic power flux in the outlet pipe for zero flow, $M = 0{\cdot}1$ and $0{\cdot}2$.

Figures 9–11 respectively show comparisons between the predicted and measured normalized acoustic power radiated from the open pipe-end for zero

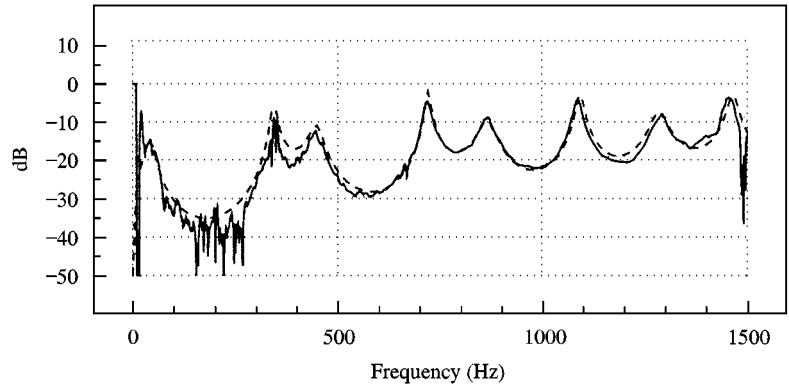

Figure 6. Measured (——) versus predicted (– – –) normalized acoustic power flux in outlet pipe with zero flow.

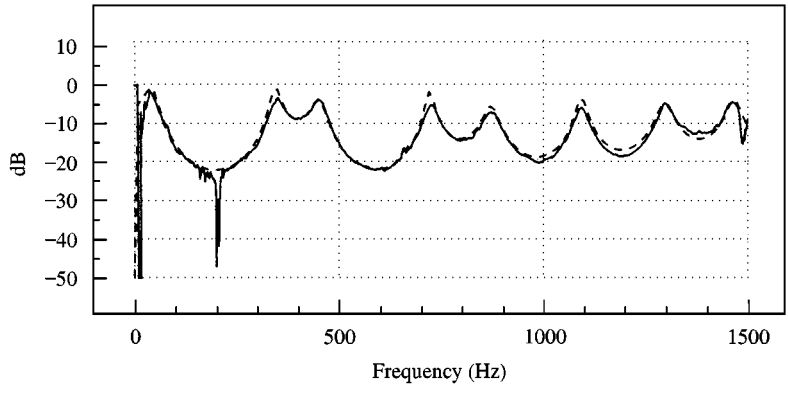

Figure 7. Measured (——) versus predicted (– – –) normalized acoustic power flux in outlet pipe with Mach number $M = 0{\cdot}1$.

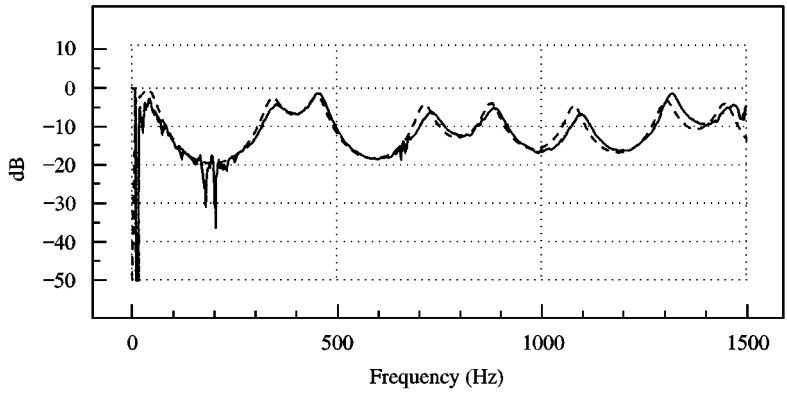

Figure 8. Measured (——) versus predicted (– – –) normalized acoustic power flux in outlet pipe with Mach number $M = 0{\cdot}2$.

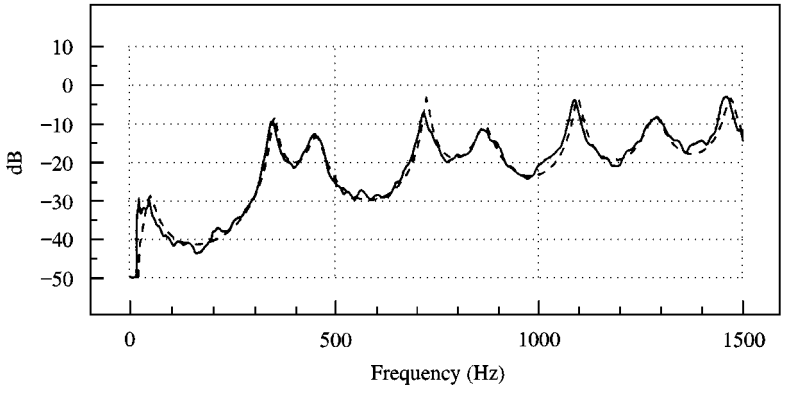

Figure 9. Measured (——) versus predicted (– – –) normalized acoustic power radiated from the open pipe-end with zero flow.

flow, $M = 0{\cdot}1$ and $M = 0{\cdot}2$. The measured radiated power was estimated from the autospectrum of the output of microphone $\#5$ (mounted at a distance r of 300 mm from, and normal to, the pipe axis and in line with the open pipe-end)

$$W_f \approx 4\pi r^2 |G_{55}|^2/\rho_0 c_0, \tag{14}$$

and the predicted radiated power was estimated [16–19] from

$$W_r = \frac{|1-R|^2}{K}\,\sigma\,\frac{[1-(KM)^2/3]}{[1+(KM)^2]^3}\,\frac{|\hat{p}^+|^2 S}{(\rho c)_{pipe}}, \tag{15}$$

where $K = c_{pipe}/c_0$, σ is the radiation efficiency and S is the cross-sectional area of the pipe.

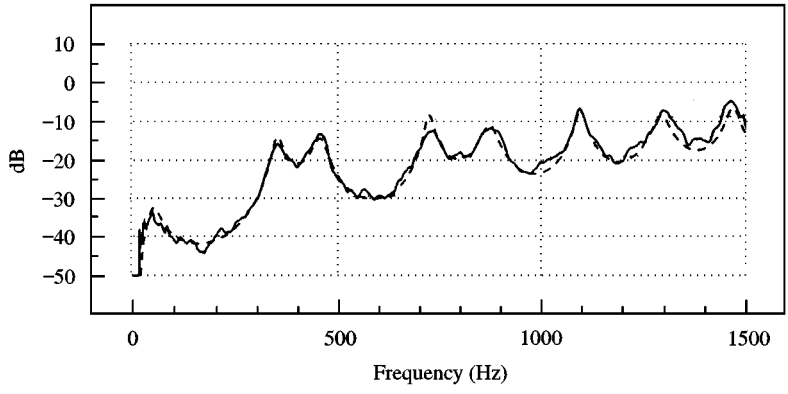

Figure 10. Measured (——) versus predicted (– – –) normalized acoustic power radiated from the open pipe-end with Mach number $M = 0{\cdot}1$.

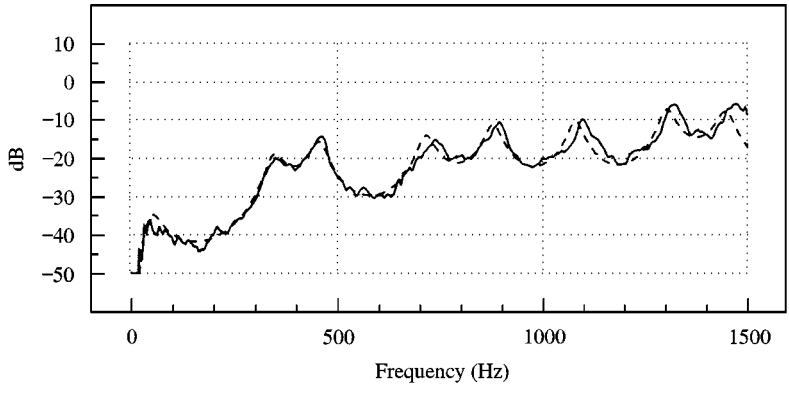

Figure 11. Measured (——) versus predicted (– – –) normalized acoustic power radiated from the open pipe-end with Mach number $M = 0{\cdot}2$.

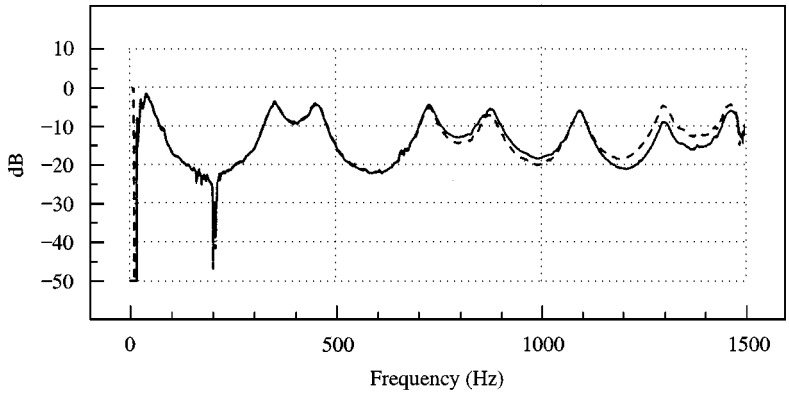

Figure 12. Comparison between the acoustic power flux in the outlet pipe with Mach number $M = 0{\cdot}1$ by using equation (11) (——) and equation (12) (– – –).

Finally, Figure 12 shows a comparison between the acoustic power flux in the outlet pipe estimated from the pressure wave components by using equations (9) and (12) with that estimated directly from the cross-spectra by using equation (11). Similar results are found except at high frequencies.

6. DISCUSSION

The measurement results presented in this paper demonstrate the problems associated with the estimation of acoustic quantities in duct systems with flow. Conventional measurement techniques using broadband excitation may yield excellent results under no-flow conditions, but the accuracy and reliability of such measurements can suffer in the presence of significant flow due to inadequate signal-to-noise ratios. Although fairly gross measurement errors may be tolerable when considering global system properties, such as pressure transfer functions, further processing of the measurements to yield estimates of (particularly) acoustic power flux reveals the need for greater precision. To the authors' knowledge, these difficulties have precluded detailed study of acoustic power flux in highly reactive duct systems to date, and as a result, much confusion surrounds topics such as acoustic sources and sinks at discontinuities.

It is shown that the signal-to-noise ratio problems can be greatly reduced by adopting a slow swept-sine technique with selective averaging. The resultant cross-spectra and transfer functions are sufficiently precise to yield reliable estimates of the nett sound power flux in a duct–even in a highly reactive sound field–provided great care is taken over *in situ* microphone calibration. One should note in passing that the success of this technique depends on the selective averaging, if a swept-sine signal is used with conventional analysis, results tend to be worse than when using random noise excitation.

Figure 3(c) shows the autospectrum of the output of microphone #1 estimated by using this technique, along with that obtained (by using conventional analysis) in the absence of acoustic excitation, that is, with the boundary layer noise alone. Somewhat surprisingly, the selective averaging technique yields values of autospectrum that are more than 10 dB below the noise floor at some frequencies; a result made possible by the exclusion of these frequencies from the averaging process when the sine-sweep frequency is away from these values. Figure 2(c), in comparison, demonstrates that the autospectrum can never drop below the noise floor with conventional analysis.

Figures 4 and 5 show comparisons between predictions of acoustic transfer functions, by using the appropriate predictive software, and measurements by using sine-sweep excitation and selective averaging. The predictions and measurements are seen to agree well for all transfer functions under all flow conditions. The "raggedness" of the measured results in Figure 5 are due to room effects; the open pipe-end was suspended at a height of some 2 m above a solid floor covered locally with acoustic wedges, the reflection from which gives rise to comb-filtering with a frequency period of approximately 85 Hz. The laboratory in which the measurements were taken also contains other experimental apparatus which further add to the unevenness of the spectrum of the output of microphone #5.

The driving force behind this investigation is the study of flow-induced acoustic sources within pipe systems. Precise measurements of nett acoustic power flux are required either side of suspected source sites to identify and quantify such sources in real systems. In this context, Figures 6–11 show comparisons between predicted and measured acoustic power flux for the system under test where the predictions and measurements are seen to agree closely. The measurement technique described herein can therefore be used in conjunction with the reliable linear predictions to study the propagation of acoustic energy through pipe systems, assuming that any significant differences between prediction and measurement can be interpreted as possibly being due to flow-induced sources or sinks, since the predictive code completely neglects their presence. The close agreement found between predictions and measurements for the current expansion chamber, where the gap between inlet and outlet pipes exceeded 10 pipe diameters, suggests that, as expected, coherent flow noise generation, if present, was hardly significant in this case; a result that was in good agreement with previous observation [5]. There were some indications, not illustrated here, of unexplained acoustic behaviour at the flow expansion into the chamber, which is the subject of a current investigation.

The raggedness of the measured result at low frequencies in Figure 6, the no-flow result, is due to the pressure reflection coefficient being very close to unity at the open pipe-end with zero flow. The phase of the transfer function between microphones $\#1$ and $\#2$ is therefore very close to zero and the nett power flux is only 0·1% or so of the total fluctuating acoustic energy in the system. Even slower sweep rates would be necessary to yield better results without flow, but luckily, the situation is improved when flow is present as demonstrated in Figures 7 and 8. These show how power flux increases with flow in accordance with equations (11) and (12).

A further benefit to the use of the selective averaging technique, not investigated at the time of writing, is the possibility of studying the propagation of individual harmonics of the excitation signal through the duct system. The technique, as described, yields results based upon the fundamental frequency of the excitation at a point in time – excluding all other frequencies – including any harmonics. It is likely that flow-induced non-linear acoustic source mechanisms, when coupled to resonant systems, may generate harmonics of the excitation frequency as well as, or instead of, the fundamental. The changes to the analysis algorithms necessary to reveal information about such harmonics are straightforward.

7. CONCLUSIONS

The swept-sine/selective averaging measurement technique described herein, along with the *in situ* calibration method, is shown to yield precise and reliable estimates of acoustic power flux within highly reactive duct systems with flow. Comparisons between the measurements and predictions from the APEX computer code, with appropriately modified output, show encouraging agreement, and it is assumed that this agreement serves to validate both the code and the measurement technique. The encouraging results open up the possibility of the detailed study of flow-induced acoustic sources in ducts.

ACKNOWLEDGMENTS

This work represents part of the studies on sources of flow-induced pressure pulsations in pipe systems transporting compressible fluids supported by Engineering and Physical Sciences Research Council Grant K79994.

REFERENCES

1. P. O. A. L. Davies and M. F. Harrison 1997 *Journal of Sound and Vibration* **202**, 249–274. Predictive acoustic modelling applied to the control of intake/exhaust noise of internal combustion engines.
2. P. O. A. L. Davies and K. R. Holland 1999 *Journal of Sound and Vibration* **223**, 425–444. I. C. engine intake and exhaust noise assessment.
3. P. O. A. L. Davies 1996 *Journal of Sound and Vibration* **190**, 345–362. Aeroacoustics and time varying systems.
4. J. C. Bruggeman, A. Hirschberg, M. E. H. Van Dongen, A. P. J. Wijnandes and J. Gorter 1991 *Journal of Sound and Vibration* **150**, 371–393. Self-sustained aeroacoustic pulsations in gas transport systems: experimental study of the influence of closed sidebranches.
5. P. O. A. L. Davies 1981 *Journal of Sound and Vibration* **77**, 191–209. Flow acoustic coupling in pipes.
6. P. A. Nelson, N. A. Halliwell and P. E. Doak 1981 *Journal of Sound and Vibration* **78**, 15–38. Fluid dynamics of flow induced resonance, Part I: experiment.
7. P. A. Nelson, N. A. Hallwell and P. E. Doak 1983 *Journal of Sound and Vibration* **91**, 375–402. Fluid dynamics of flow induced resonance, Part II: flow acoustic interaction.
8. T. D. Mast and A. D. Pierce 1995 *Journal of the Acoustic Society of America* **97**, 163–172. Describing function theory for flow excited resonators.
9. P. O. A. L. Davies, M. Bhattacharya and J. L. Bento Coelho 1980 *Journal of Sound and Vibration* **72**, 539–542. The measurement of plane wave acoustic fields in flow ducts.
10. J. Y. Chung and D. A. Blaser 1980 *Journal of the Acoustic Society of America* **68**, 1570–1577. Transfer function method of measuring acoustic intensity in a duct system with flow.
11. E. Dokumaci 1997 *Journal of Sound and Vibration* **208**, 653–655. A note on the transmission of sound in a wide pipe with mean flow and viscothermal attenuation.
12. F. J. Fahy 1989 *Sound Intensity*. London: Elsevier Science Publishers Ltd., Chapter 9. ISBN 1-85166-319-3.
13. C. L. Morfey 1971 *Journal of Sound and Vibration* **14**, 37–55. Sound generation and transmission in ducts with flow.
14. H. Bodén and M. Åbom 1986 *Journal of the Acoustic Society of America* **79**, 541–549. Influence of errors on the two-microphone method for measuring acoustic properties in ducts.
15. P. O. A. L. Davies, M. F. Harrison and H. J. Collins 1997 *Journal of Sound and Vibration* **200**, 195–225. Acoustic modelling of multiple path silencers with experimental validations.
16. R. M. Munt 1977 *Journal of Fluid Mechanics*, **83**, 609–640. The interaction of sound with a subsonic jet issuing from a semi-infinite cylindrical pipe.
17. A. M. Cargill 1979 *Mechanics of Sound Generation in Flows*, 19–25. Berlin: Springer.
18. P. O. A. L. Davies and R. F. Halliday 1981 *Journal of Sound and Vibration* **76**, 591–594. Radiation of sound by a hot exhaust.
19. R. M. Munt 1990 *Journal of Sound and Vibration* **142**, 413–436. Acoustic transmission properties of a jet pipe with subsonic jet flow: I, the cold jet reflection coefficient.